IJMSO

International Journal of Mathematical Sciences and Optimization: Theory and Applications
11(3), 2025, Pages 88 - 107
https://doi.org/10.5281/zenodo.17604615

Quantifying the Public Health Effects of Vaccine Hesitancy and Delays in Screening Clinically Infected Patients: Insights From a COVID-19 Transmission Model

Paride O. Lolika [1*], Mlyashimbi Helikumi [2], Kenneth Sube [3], Steady Mushayabasa [4]

1. Department of Mathematics, University of Juba, P.O. Box 82 Juba, South Sudan.
2. Department of Mathematics and Statistics, Mbeya University of Science and Technology, College of Science and Technical Education, P.O. Box 131, Mbeya, Tanzania.
3. Department of Ophthalmology, University of Juba P.O. Box 82 Juba, South Sudan.
4. Department of Mathematics and Computational Sciences, University of Zimbabwe, P.O. Box MP 167, Mount Pleasant, Harare, Zimbabwe.
* Corresponding author: parideoresto@yahoo.com[1], mhelikumi@yahoo.co.uk, ladolojuan@gmail.com, steadymushaya@gmail.com

Article Info
Received: 14 May 2025 Revised: 11 July 2025
Accepted: 20 September 2025 Available online: 10 October 2025

Abstract

Motivated by the recent COVID-19 outbreak, we develop a time delay infectious disease model that incorporates vaccination and screening of clinically infected patients and calibrate it using Chinese data to understand the quantitative implications of vaccine hesitancy and delay in the screening of clinically infected patients. Vaccine hesitancy refers to the denial or delay in acceptance of vaccines despite their availability. Understanding the implications of vaccine hesitancy is therefore essential for designing public health interventions. Analysis of the model revealed that whenever $\mathcal{R}_0 \leq 1$, there exists a globally asymptotically disease-free equilibrium. However, whenever $\mathcal{R}_0 > 1$, there exists a unique endemic equilibrium which is globally asymptotically stable. In addition, results also show that vaccine hesitancy and delay in hospitalizing clinically infected patients have a stronger impact on the deaths toll and new infections generated [1,2]. Vaccine hesitancy and delayed screening of clinically infected patients lead to harmonic oscillations in deaths and new cases, which, however, die out over time. Our findings underscore the importance of including vaccine hesitancy and delay in hospitalizing clinically infected patients in the design of control strategies for infectious diseases.

Keywords: Coronavirus, Mathematical Model, Time Delay, Vaccine Hesitancy, Screening Delay.
MSC2010: 65M06, 65N35, 35F50.

1 Introduction

Since the introduction of various COVID-19 vaccines, a significant portion of the global population has expressed reluctance to receive vaccinations, a phenomenon known as vaccine hesitancy [1,3,4].

IJMSO

International Journal of Mathematical Sciences and Optimization: Theory and Applications
11(3), 2025, Pages 88 - 107
https://doi.org/10.5281/zenodo.17604615

The World Health Organization (WHO) defines vaccine hesitancy as the delay in acceptance or outright refusal of vaccines, even when vaccination services are available [5]. This hesitancy can undermine the overall efficacy of vaccination efforts [6, 7]. Empirical studies indicate that average acceptance rates for COVID-19 vaccines remain relatively low worldwide, with a global pooled acceptance rate of 60.23% [5, 8]. While a 2023 survey showed an increase in acceptance across 23 countries, hesitancy increased in others [5]. Regions such as the Middle East, Russia, Africa, and several European countries report particularly low acceptance rates [5, 9]. For instance, a study conducted in France in October 2020 found that 46% of French citizens were hesitant about vaccination. Other studies reveal significant hesitancy rates: 36% in Spain and the USA, 35% in Italy, 32% in South Africa, and 31% in Japan and Germany [5]. Several factors contribute to this hesitancy, including a lack of information regarding side effects especially long-term effects concerns about the vaccine development timeline, cultural and religious beliefs, political influences, and the spread of misinformation and conspiracy theories [4, 7]. Misinformation, disinformation, and the "infodemic" have significantly contributed to vaccine hesitancy and lower rates [7]. A 2025 study identified demographic, psychological, and behavioral factors as drivers of increased hesitancy for booster doses [7]. Factors such as structural and socioeconomic inequalities, lack of effective public health messaging, and unethical research also play a role [4]. Given these substantial rates of hesitancy and refusal regarding COVID-19 vaccinations, it is essential to quantify the public health implications of vaccine hesitancy on the dynamics of COVID-19 transmission. Delays in screening clinically infected individuals with COVID-19 also pose significant risks to public health by facilitating virus transmission, worsening individual health outcomes, straining healthcare systems, complicating public health responses, and causing psychosocial distress [10, 11]. Delayed diagnoses can lead to more severe cases, increased hospitalizations, and higher mortality rates [10, 12]. The potential for increased transmission due to delayed screening necessitates stricter control measures and broader testing to mitigate further spread [11]. Moreover, delayed screening can exacerbate existing health disparities, disproportionately affecting vulnerable populations [13, 14]. Although vaccination and screening of infectious individuals remain important disease control strategies, their implementation is not instantaneous. Delays in vaccination may occur due to the unavailability of vaccines or refusal of individuals to accept available vaccines, while delays in screening of infectious individuals may occur due to limited medical resources such as the unavailability of diagnostic testing kits [1, 2]. However, from a public-health perspective, delays in vaccination and screening of clinically infected individuals are major sources of morbidity and mortality [2]. Therefore, understanding the quantitative public health impact of vaccine hesitancy and the delays in screening clinically infected patients is important for designing public health interventions [11, 13, 14]. In this context, this work aims to quantitatively assess the influence of vaccine hesitancy and delays in the screening of clinically infected patients on the evolution of an infectious disease through a mathematical model. In epidemiology, mathematical models have proven to be powerful tools capable of generating a deeper understanding of the mechanisms underlying the disease spread process, as well as to support decision makers in planning and implementing control measures [15, 16]. Motivated by the recent COVID-19 outbreak, our dynamical model will be based on the epidemiology of this disease. In particular, the recent COVID-19 outbreak was marked by significant vaccine hesitancy and delays in screening of infectious individuals [17, 18]. During the spread of COVID-19, various mathematical models were developed to understand, explain, assess the impact of control strategies, and predict disease evolution (see, for example [19–22]). The studies in [19–22]) and those cited therein produced useful results. For instance, Lu et al. [19] employed a system of delay differential equations (DDEs) to evaluate how recovery delays in infectious individuals affect transmission dynamics. They found that small changes in the time delay factor lead to large changes in disease dynamics, while a large delay factor leads to oscillatory disease dynamics.

Similarly, Albani et al. [20] utilized COVID-19 data from Chicago and New York City to develop a mathematical model assessing the impact of vaccination delays on COCVID-19 dynamics. Their analysis indicated that the earlier a vaccination campaign begins, the greater its potential impact in reducing COVID-19 cases and deaths. This underscores the importance of timely vaccination efforts in controlling outbreaks. Furthermore, Yang [21] assessed the implications of hierarchical

IJMSO

International Journal of Mathematical Sciences and Optimization: Theory and Applications
11(3), 2025, Pages 88 - 107
https://doi.org/10.5281/zenodo.17604615

quarantine with delay, providing valuable insights into how delayed interventions can affect the overall effectiveness of quarantine measures. The study revealed that delaying the detection and quarantine of infectious individuals may lead to disease outbreaks. Together, these studies illustrate the significant influence of timing in both recovery and intervention strategies on the trajectory of COVID-19, emphasizing the need for prompt action to mitigate its impact. Despite these efforts, however, prior studied do not address the combined effects of vaccine hesitancy and delaying the screening of clinically infected patients on the evolution of an infectious disease remain poorly understood. Motivation for our study on modelling of COVID-19 stems from the pressing issues of post-pandemic vaccine fatigue and delays in variant screening. Understanding the public health impact of vaccine hesitancy and delays in screening of infectious individuals is essential for policymakers to decide how and when to deploy control measures [11, 13, 14]. To that end, this study aims to fill this gap by developing and analyzing a new mathematical model for COVID-19 governed by delay differential equations (DDEs). Models based on DDEs can capture the effects of vaccine hesitancy and delays in the screening of clinically infected patients. Thus, the proposed model has two-timed delay factors, namely τ_1 and τ_2 accounts for the time taken by susceptible unvaccinated individuals to decide on vaccination after receiving information (vaccine hesitancy) and the time gap between when an infection begin and when a patient is diagnosed or screen (delays in screening of clinically infected patients), respectively [23]. In addition, we also assume that vaccinated individuals have a reduced risk of contracting the disease compared to unvaccinated.

This paper is outlined as follows. In Section 2, we introduce the methods and analytical findings of the study. We compute the reproduction number and investigate the stability of the model's steady states. Simulation results validating the model and analyzing threshold accuracy are presented in Section 3. The paper concludes with a brief summary of the findings.

2 Methods and analytical Results

2.1 Mathematical model

To understand the implications of vaccine hesitancy and delay of screening infectious individuals on the transmission and control of COVID-19, we propose a population-based mathematical model that subdivides the total human population at time t into compartments of: susceptible high-risk (unvaccinated) individuals $S_H(t)$, susceptible low-risk (vaccinated) individuals $S_L(t)$. The high-risk susceptible individuals are those that are unvaccinated human with underlying medical conditions demonstrated to have a high risk of death due to COVID-19 [24], as well as the elderly [25], the low-risk susceptible population includes those that are not in $S_H(t)$. Exposed/latent individuals $E(t)$, symptomatic infectious individuals, $I_s(t)$, asymptomatic infectious individuals $I_a(t)$, hospitalized patients $Q(t)$, recovered individuals $R(t)$ and Deceased $D(t)$. The dynamics of these compartments are summarized by the following system of equations:

$$
\begin{aligned}
S_H'(t) &= \Lambda - \lambda(t)S_H(t) - (\mu+\sigma)S_H(t), && (2.1)\\
S_L'(t) &= \sigma e^{-\mu\tau_1}S_H(t-\tau_1) - (1-\phi)\lambda(t)S_L(t) - \mu S_L(t), && (2.2)\\
E'(t) &= \lambda(t)(S_H(t) + (1-\phi)S_L(t)) - (\mu+\alpha)E(t), && (2.3)\\
I_s'(t) &= p\alpha E(t) - (\mu + r_1 + \gamma_1 + d_1)I_s(t), && (2.4)\\
I_a'(t) &= (1-p)\alpha E(t) - (\mu + r_2 + \gamma_2)I_a(t), && (2.5)\\
Q'(t) &= \gamma_1 e^{-(\mu+d_1)\tau_2}I_s(t-\tau_2) + \gamma_2 e^{-\mu\tau_2}I_a(t-\tau_2) - (\mu + d_2 + \delta)Q(t), && (2.6)\\
R'(t) &= r_1 I_s(t) + r_2 I_a(t) + \delta Q(t) - \mu R(t), && (2.7)\\
D'(t) &= d_1 I_s(t) + d_2 Q(t), && (2.8)
\end{aligned}
$$

where all parameters are positive constants and defined as follows: Λ is the recruitment rate; β is the disease transmission rate; ψ $(0 \leq \psi < 1)$ accounts for the reduction of infectivity of the asymptomatic infectious patients relative to other infectious individuals. Similarly, ρ $(0 \leq \rho < 1)$

IJMSO
International Journal of Mathematical Sciences and Optimization: Theory and Applications
11(3), 2025, Pages 88 - 107
https://doi.org/10.5281/zenodo.17604615

models the reduction of infectivity of quarantined individuals relative to other infectious individuals. μ is the natural mortality rate, σ is the vaccination rate, the term $\sigma e^{-\mu\tau_1} S_H(t-\tau_1)$ represents the individuals surviving in the vaccinated class (low risk) (see for example [26]), τ_1 accounts for the time taken by susceptible unvaccinated individuals to accept the vaccine despite its availability (vaccine hesitancy), τ_2 refer to the time gap between when an infection begin and when a patient is diagnosed or screen (delay in screening), $1/\alpha$ is the incubation period, p $(0 < p < 1)$ denotes a fraction of infected individuals who develop clinical signs of the disease, ϕ $(0 \leq \phi < 1)$ represents vaccine efficacy, r_1 and r_2 model the recovery of non-hospitalized symptomatic infectious and asymptomatic infectious individuals, respectively, γ_1 and γ_2 account for the detection and hospitalization of symptomatic infectious and asymptomatic infectious individuals, respectively, d_1 and d_2 denotes disease-related deaths of symptomatic infectious patients and quarantined individuals, respectively, hospitalized patients recover after $1/\delta$ days. The model flow diagram is depicted in Fig. (1).
Additional biological and epidemiological assumptions that govern the model (2.1)-(2.8) are:

(i) All new recruits are assumed to be susceptible high risk and unvaccinated and recruited at the rate Λ. Thus consider the following force of infection $\lambda(t) = \beta(I_s(t)+(1-\psi)I_a(t)+(1-\sigma)Q(t))$, where β is the infection rate and $(1-\psi)$ accounts for the reduction of infectivity of the asymptomatic infectious patients relative to other infectious individuals. Similarly, $(1-\rho)$ models the reduction of infectivity of quarantined individuals relative to other infectious individuals.

(ii) Susceptible high risk and susceptible low risk are assumed to acquire infection following effective contact with symptomatic infectious individuals, $I_s(t)$, asymptomatic infectious individuals $I_a(t)$, and hospitalized patients $Q(t)$,

(iii) Upon being infected with COVID-19, individuals enter the exposed state.

(iv) We assume that death only comes from symptomatic infectious and quarantined, not from asymptomatic.

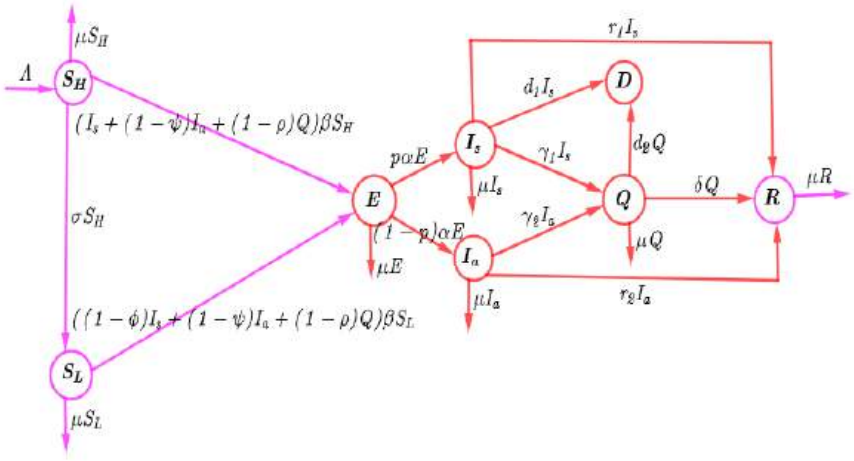

Figure 1: Model flow chat illustrating the dynamics of COVID-19

For biological relevance, the initial conditions for system (2.1)-(2.8), take the form (2.9):

$$\begin{aligned} S_H(\theta) &= \varphi_1(\theta), \quad S_L(\theta) = \varphi_2(\theta), \quad E(\theta) = \varphi_3(\theta), \quad I_s(\theta) = \varphi_4(\theta), \\ I_a(\theta) &= \varphi_5(\theta), \quad Q(\theta) = \varphi_6(\theta), \quad R(\theta) = \varphi_7(\theta), D(\theta) = \varphi_8(\theta), \quad \theta \in [-\tau, 0], \quad \tau > 0, \end{aligned} \tag{2.9}$$

IJMSO
International Journal of Mathematical Sciences and Optimization: Theory and Applications
11(3), 2025, Pages 88 - 107
https://doi.org/10.5281/zenodo.17604615

where $\tau = \max\{\tau_1, \tau_2\}$ and $(\varphi_1(\theta), \varphi_2(\theta), \varphi_3(\theta), \varphi_4(\theta), \varphi_5(\theta), \varphi_6(\theta), \varphi_7(\theta), \varphi_8(\theta)) \in C([-\tau, 0], \mathbb{R}^8_+)$ is the Banach space of continuous functions mapping the interval $[-\tau, 0]$ into $\mathbb{R}^8_+$, and $\mathbb{R}^8+ = \{(x_1, x_2, ..., x_8) : x_i \geq 0, i = 1, ..., 8\}$. It follows, from the fundamental theory of functional differential equations [27], that system (2.1)-(2.8) has a unique solution ($S_H(t)$, $S_L(t)$, $E(t)$, $I_s(t)$, $I_a(t)$, $Q(t)$, $R(t)$, $D(t)$) that satisfies the initial conditions (2.9). One can easily verify that all the solutions of model (2.1)-(2.8) with the initial conditions (2.9) are defined on $[0, \infty)$ and they are always positive for all $t \geq 0$ and are bounded and lie in the region Ω which is a positively invariant set with respect to system (2.1)-(2.8), where the feasible region Ω is given by $\Omega = \{(S_H \geq 0, S_L \geq 0, E \geq 0, I_s \geq 0, I_a \geq 0, Q \geq 0, R \geq 0, D \geq 0) : S_H + S_L + E + I_s + I_a + Q + R + D \leq \Lambda/\mu\}$.

2.2 The reproduction number

In epidemiological models, the strength of the disease to invade the population is measured by the reproduction number. It is commonly defined as the expected number of secondary infections generated by a single infectious individual during their entire infectious period in a population of wholly susceptible individuals. Through direct calculations, one can observe that system (2.1)-(2.8) has a disease-free equilibrium (DFE) given $\mathcal{E}^0 : (S_H^0, S_L^0, 0, 0, 0, 0)$, where $S_H^0 = \frac{\Lambda}{(\mu+\sigma)}$, and $S_L^0 = \frac{\Lambda\sigma e^{-\mu\tau_1}}{\mu(\mu+\sigma)}$. Following the next-generation matrix method [28], we define the nonnegative matrix $\mathcal{F}$ that represents the generation of new infection terms and the matrix $\mathcal{V}$ which accounts for the remaining transfer terms, evaluated at DFE, respectively as follows (2.10):

$$\mathcal{F} = \begin{bmatrix} 0 & \beta(S_H^0 + (1-\phi)S_L^0) & \beta(1-\psi)(S_H^0 + (1-\phi)S_L^0) & \beta(1-\rho)(S_H^0 + (1-\phi)S_L^0) \\ 0 & 0 & 0 & 0 \\ 0 & 0 & 0 & 0 \\ 0 & 0 & 0 & 0 \end{bmatrix},$$

$$\mathcal{V} = \begin{bmatrix} \mu+\alpha & 0 & 0 & 0 \\ -p\alpha & \mu + r_1 + \gamma_1 + d_1 & 0 & 0 \\ -(1-p)\alpha & 0 & \mu + r_2 + \gamma_2 & 0 \\ 0 & -\gamma_1 e^{-(\mu+d_1)\tau_2} & -\gamma_2 e^{-\mu\tau_2} & \mu + d_2 + \delta \end{bmatrix}. \tag{2.10}$$

From (2.10), it follows that the spectral radius of system (2.1)-(2.8) is (2.11):

$$\begin{aligned} \mathcal{R}_0 &= \frac{\beta p\alpha}{(\mu+\alpha)(\mu + r_1 + \gamma_1 + d_1)}\left(\frac{\Lambda}{(\mu+\sigma)} + (1-\phi)\frac{\Lambda\sigma e^{-\mu\tau_1}}{\mu(\mu+\sigma)}\right) \\ &\quad + \frac{\beta(1-p)(1-\psi)\alpha}{(\mu+\alpha)(\mu + r_2 + \gamma_2)}\left(\frac{\Lambda}{(\mu+\sigma)} + (1-\phi)\frac{\Lambda\sigma e^{-\mu\tau_1}}{\mu(\mu+\sigma)}\right) \\ &\quad + \frac{\beta\alpha(1-\rho)}{(\mu+\alpha)(\mu + d_2 + \delta)}\left(\frac{p\gamma_1 e^{-(\mu+d_1)\tau_2}}{\mu + r_1 + \gamma_1 + d_1} + \frac{(1-p)\gamma_2 e^{-\mu\tau_2}}{\mu + r_2 + \gamma_2}\right) \\ &\quad \times \left(\frac{\Lambda}{(\mu+\sigma)} + (1-\phi)\frac{\Lambda\sigma e^{-\mu\tau_1}}{\mu(\mu+\sigma)}\right) \\ &= \mathcal{R}_{0s} + \mathcal{R}_{0a} + \mathcal{R}_{0q}. \end{aligned} \tag{2.11}$$

The quantities, $\mathcal{R}_{0s}$, $\mathcal{R}_{0s}$ and $\mathcal{R}_{0q}$ represents the expected number of secondary infections generated by symptomatic, asymptomatic and hospitalized infectious patients during their entire infectious period in a population of vaccinated and unvaccinated susceptible individuals. In Eq. (2.11) $\frac{\Lambda}{(\mu+\sigma)} + (1-\phi)\frac{\Lambda\sigma e^{-\mu\tau_1}}{\mu(\mu+\sigma)}$ represents the population susceptible individuals (vaccinated and unvaccinated) who can contract the disease after effective contact with infectious individuals, $\frac{\alpha}{\mu+\alpha}$ is probability of latently infected individuals to survive this state and become infectious. A proportion p of the exposed individuals who survive this state will become symptomatic infectious patients for an

IJMSO

International Journal of Mathematical Sciences and Optimization: Theory and Applications
11(3), 2025, Pages 88 - 107
https://doi.org/10.5281/zenodo.17604615

average duration of $\frac{1}{\mu+r_1+\gamma_1+d_1}$ and the remainder, $(1-p)$ will become asymptomatic infectious patients for an average duration of $\frac{1}{\mu+r_2+\gamma_2}$. Symptomatic and asymptomatic infectious patients are detected at rates γ_1 and γ_2, respectively, and their survival rate in this state is given by $e^{-(\mu+d_1)\tau_2}$ and $e^{-\mu\tau_2}$. In addition, detected and hospitalized patients will be infectious for an average period of $\frac{1}{\mu+d_2+\delta}$.

2.3 Stability of model steady states

In this section, we study the stability of the model's steady states. We will investigate the global stability of the DFE and the endemic equilibrium. Since equations (2.7) and (2.8) do not contribute to the generation of new infections, it suffices to neglect these equations when investigating the stability of the model's steady states. We commence by claiming the following results.

Theorem 2.1. *For any $\tau_1 \geq 0, \tau_2 \geq 0$, the DFE of system (2.1)-(2.8) is globally asymptotically stable if $\mathcal{R}_0 < 1$.*

Proof. Let us consider a Lyapunov functional (2.12):

$$\begin{aligned} W_0(t) &= \left[S_H - S_H^0 - S_H^0 \ln\left(\frac{S_H}{S_H^0}\right)\right] + \left[S_L - S_L^0 - S_L^0 \ln\left(\frac{S_L}{S_L^0}\right)\right] \\ &\quad + a_1 E(t) + a_2 I_s(t) + a_3 I_a(t) + a_4 Q(t) + \sigma\left(1 - \frac{S_L^0}{S_L}\right)\int_{t-\tau_1}^{t} S_H(\theta)d\theta \\ &\quad + \gamma_1 e^{-(\mu+d_1)\tau_2}\int_{t-\tau_2}^{t} I_s(\theta)d\theta + \gamma_2 e^{-\mu\tau_2}\int_{t-\tau_2}^{t} I_a(\theta)d\theta, \end{aligned} \tag{2.12}$$

where:

$$\left.\begin{aligned} a_1 &= \frac{\beta p\alpha}{m_1 m_2} + \frac{\beta(1-p)(1-\psi)\alpha}{m_1 m_3} + \frac{\beta(1-\rho)p\alpha\gamma_1 e^{-(\mu+d_1)\tau_2}}{m_1 m_2 m_4} + \frac{\beta(1-\rho)(1-p)\alpha\gamma_2 e^{-\mu\tau_2}}{m_1 m_3 m_4}, \\ a_2 &= \frac{\beta}{m_2} + \frac{\beta(1-\rho)\gamma_1 e^{-(\mu+d_1)\tau_2}}{m_2 m_4}, \quad a_3 = \frac{\beta(1-\psi)}{m_3} + \frac{\beta(1-\rho)\gamma_2 e^{-\mu\tau_2}}{m_3 m_4}, \quad a_4 = \frac{\beta(1-\rho)}{m_4}, \end{aligned}\right\} \tag{2.13}$$

with:

$$\left.\begin{aligned} m_1 &= (\mu+\alpha), \quad m_2 = (\mu + r_1 + \gamma_1 + d_1), \\ m_3 &= (\mu + r_2 + \gamma_2), \quad m_4 = (\mu + d_2 + \delta). \end{aligned}\right\} \tag{2.14}$$

Taking the derivative of $W_0(t)$ along the solutions system (2.1)-(2.8) and making some algebraic simplification one gets:

$$\begin{aligned} W_0'(t) &\leq \Lambda\left(2 - \frac{S_H(t)}{S_H^0} - \frac{S_H^0}{S_H(t)}\right) + \sigma S_H^0\left(3 - \frac{S_H^0}{S_H(t)} - \frac{S_H(t)S_L^0}{S_H^0 S_L(t)} - \frac{S_L(t)}{S_L^0}\right) \\ &\quad + \beta(\mathcal{R}_0 - 1)(I_s(t) + (1-\psi)I_a(t) + (1-\rho)Q(t)). \end{aligned} \tag{2.15}$$

If $\mathcal{R}_0 \leq 1$, then $W_0'(t) \leq 0$, since $2 - \frac{S_H}{S_H^0} - \frac{S_H^0}{S_H} \leq 0$, and $3 - \frac{S_H^0}{S_H} - \frac{S_H S_L^0}{S_H^0 S_L} - \frac{S_L}{S_L^0} \leq 0$. Let M be the largest invariant set in Ω, we can observe that $W_0'(t) = 0$ if either $\mathcal{R}_0 = 1$ or $S_H^0 = S_H$, and $S_L^0 = S_L$. Therefore, by the Lyapunov-LaSalle invariance principle [29], the DFE is globally asymptotically stable whenever $\mathcal{R}_0 \leq 1$. This completes the proof. □

We now proceed to establish the existence of the endemic equilibrium. We claim the following results.

Theorem 2.2. *If $\mathcal{R}_0 > 1$, then system (2.1)-(2.8) admits a unique endemic equilibrium point.*

Proof. Let us denote any non-trivial equilibrium of system (2.1)-(2.8) by $\mathcal{E}^* = (S_H^*, S_L^*, E^*, I_s^*, I_a^*, Q^*)$, where:

$$S_H^* = \frac{\Lambda}{(\mu + \sigma + m_0 E^*)}, \qquad S_L^* = \frac{\sigma e^{-\mu\tau_1}\Lambda}{(\mu + (1-\phi)m_0 E^*)(\mu + \sigma + m_0 E^*)},$$

IJMSO
International Journal of Mathematical Sciences and Optimization: Theory and Applications
11(3), 2025, Pages 88 - 107
https://doi.org/10.5281/zenodo.17604615

$$I_s^* = \frac{p\alpha E^*}{m_2}, \quad I_a^* = \frac{(1-p)\alpha E^*}{m_3}, \quad Q^* = \left(\frac{p\alpha\gamma_1 e^{-(\mu+d_1)\tau_2}}{m_2 m_4} + \frac{(1-p)\alpha\gamma_2 e^{-\mu\tau_2}}{m_3 m_4}\right)E^*,$$

with:

$$m_0 = \beta\left[\frac{p\alpha}{m_2} + \frac{(1-p)(1-\psi)\alpha}{m_3} + (1-\rho)\left(\frac{p\alpha\gamma_1 e^{-(\mu+d_1)\tau_2}}{m_2 m_4} + \frac{(1-p)\alpha\gamma_2 e^{-\mu\tau_2}}{m_3 m_4}\right)\right]. \quad (2.16)$$

From equation (2.3) we have

$$E = \frac{m_0}{m_1} g(E) E, \quad (2.17)$$

where $g(E) = S_H(E) + (1-\phi)S_L(E)$. From equation (2.17) with $E \neq 0$, it follows that for an endemic equilibrium to exist we must have:

$$g(E) = \frac{m_1}{m_0}. \quad (2.18)$$

Clearly, $g(E)$ is differentiable for all $E > 0$. Differentiating $g(E)$ leads to:

$$\begin{aligned} g'(E) &= \frac{\partial g}{\partial S_H}\frac{\partial S_H}{\partial E} + \frac{\partial g}{\partial S_L}\frac{\partial S_L}{\partial E} \\ &= -\frac{\Lambda m_0}{(\mu+\sigma+m_0E)^2} - \frac{\sigma e^{-\mu\tau_1}\Lambda m_0}{(\mu+(1-\phi)m_0E)(\mu+\sigma+m_0E)^2} \\ &\quad -\frac{\sigma e^{-\mu\tau_1}(1-\phi)\Lambda m_0}{(\mu+\sigma+m_0E)(\mu+(1-\phi)m_0E)^2}. \\ &= -\frac{\Lambda m_0}{(\mu+\sigma+m_0E)^2}\left(1 + \frac{\sigma e^{-\mu\tau_1}}{(\mu+(1-\phi)m_0E)} + \frac{\sigma e^{-\mu\tau_1}(1-\phi)(\mu+\sigma+m_0E)}{(\mu+(1-\phi)m_0E)^2}\right) \quad (2.19) \end{aligned}$$

From equation (2.19) with $E \geq 0$, it implies that $g(E)$ is a decreasing curve on $[0,\infty)$ since $g'(E) < 0$. To determine if the function $g(E)$ intersects the constant function on the right-hand side of equation (2.18), we must investigate $g(0)$. Since $g(0) = S_H(0) + (1-\phi)S_L(0) = \frac{\Lambda}{(\mu+\sigma)} + (1-\phi)\frac{\Lambda\sigma e^{-\mu\tau_1}}{\mu(\mu+\sigma)}$, one can express $\mathcal{R}_0$ as follows $\mathcal{R}_0 = \frac{m_0}{m_1}g(0)$. Thus, whenever $\mathcal{R}_0 > 1$, then $g(E) > \frac{m_1}{m_0}$, and there is a unique endemic equilibrium $E = E^* > 0$. However, if $\mathcal{R}_0 \leq 1$, then $g(E) \leq \frac{m_1}{m_0}$ and there is no endemic equilibrium. □

Next, we investigate the global stability of the endemic equilibrium $\mathcal{E}^*$. We claim the following results.

Theorem 2.3. *If $\mathcal{R}_0 > 1$, the unique endemic equilibrium of system (2.1)-(2.8) is globally asymptotically stable.*

Proof. Let us consider the following Lyapunov functional (2.20):

$$\begin{aligned} W_1(t) &= b_1\left\{S_H - S_H^* - S_H^*\ln\left(\frac{S_H}{S_H^*}\right)\right\} + b_2\left\{S_L - S_L^* - S_L^*\ln\left(\frac{S_L}{S_L^*}\right)\right\} \\ &\quad + b_3\left\{E - E^* - E^*\ln\left(\frac{E}{E^*}\right)\right\} + b_4\left\{I_s - I_s^* - I_s^*\ln\left(\frac{I_s}{I_s^*}\right)\right\} \\ &\quad + b_5\left\{I_a - I_a^* - I_a^*\ln\left(\frac{I_a}{I_a^*}\right)\right\} + b_6\left\{Q - Q^* - Q^*\ln\left(\frac{Q}{Q^*}\right)\right\} \\ &\quad + b_2\sigma\left(1 - \frac{S_L^*}{S_L}\right)\int_{t-\tau_1}^{t} S_H(\theta)d\theta + b_6\gamma_1 e^{-(\mu+d_1)\tau_2}\int_{t-\tau_2}^{t}\left(1 - \frac{Q^*}{Q}\right)I_s(\theta)d\theta \\ &\quad + b_6\gamma_2 e^{-\mu\tau_2}\left(1 - \frac{Q^*}{Q}\right)\int_{t-\tau_2}^{t} I_a(\theta)d\theta, \end{aligned} \quad (2.20)$$

IJMSO
International Journal of Mathematical Sciences and Optimization: Theory and Applications
11(3), 2025, Pages 88 - 107
https://doi.org/10.5281/zenodo.17604615

with

$$
\begin{aligned}
b_1 &= b_2 = b_3 = 1,\\
b_4 &= \frac{\beta(1-\psi)I_a^*(S_H^*+(1-\phi)S_L^*)}{(1-p)\alpha E^*} + \frac{\beta(1-\psi)(1-\rho)\gamma_2 e^{-\mu\tau_2}I_a^*Q^*}{(1-p)\alpha E^*}\left(\frac{S_H^*+(1-\phi)S_L^*}{\gamma_1 e^{-(\mu+d_1)}I_s^*+\gamma_2 e^{-\mu\tau_2}I_a^*}\right),\\
b_5 &= \frac{\beta I_s^*(S_H^*+(1-\phi)S_L^*)}{p\alpha E^*} + \frac{\beta(1-\rho)\gamma_1 e^{-(\mu+d_1)\tau_2}I_s^*Q^*}{p\alpha E^*}\left(\frac{S_H^*+(1-\phi)S_L^*}{\gamma_1 e^{-(\mu+d_1)\tau_2}I_s^*+\gamma_2 e^{-\mu\tau_2}I_a^*}\right),\\
b_6 &= \frac{\beta(1-\rho)Q^*(S_H^*+(1-\phi)S_L^*)}{\gamma_1 e^{-(\mu+d_1)\tau_2}I_s^*+\gamma_2 e^{-\mu\tau_2}I_a^*}.
\end{aligned}
\tag{2.21}
$$

After some algebraic manipulations, one gets (2.22):

$$
\begin{aligned}
W_1'(t) &= (\mu+\sigma)S_H^*\left(2-x_1-\frac{1}{x_1}\right)+\mu S_L^*\left(3-\frac{x_1}{x_2}-\frac{1}{x_1}-x_2\right)\\
&+\beta(1-\psi)I_a^*S_H^*\left(3-\frac{1}{x_1}-\frac{x_3}{x_4}-\frac{x_4}{x_3}x_1\right)+\beta I_s^*S_H^*\left(3-\frac{1}{x_1}-\frac{x_3}{x_5}-\frac{x_5}{x_3}x_1\right)\\
&+\frac{\beta(1-\psi)(1-\rho)\gamma_2 I_a^*Q^*S_H^*}{\gamma_1 e^{-(\mu+d_1)\tau_2}I_s^*+\gamma_2 e^{-\mu\tau_2}I_a^*}\left(4-\frac{1}{x_1}-\frac{x_3}{x_4}-\frac{x_4}{x_6}-\frac{x_6}{x_3}x_1\right)\\
&+\beta(1-\psi)(1-\phi)I_a^*S_L^*\left(4-\frac{1}{x_1}-\frac{x_1}{x_2}-\frac{x_3}{x_4}-\frac{x_4}{x_3}x_2\right)\\
&+\beta(1-\phi)I_s^*S_L^*\left(4-\frac{1}{x_1}-\frac{x_1}{x_2}-\frac{x_3}{x_5}-\frac{x_5}{x_3}x_2\right)\\
&+\frac{\beta(1-\rho)\gamma_1 e^{-(\mu+d_1)}I_s^*Q^*S_H^*}{\gamma_1 e^{-(\mu+d_1)\tau_2}I_s^*+\gamma_2 e^{-\mu\tau_2}I_a^*}\left(4-\frac{1}{x_1}-\frac{x_3}{x_5}-\frac{x_5}{x_6}-\frac{x_6}{x_3}x_1\right)\\
&+\frac{\beta(1-\psi)(1-\rho)(1-\phi)\gamma_2 e^{-\mu\tau_2}I_a^*Q^*S_L^*}{\gamma_1 e^{-(\mu+d_1)\tau_2}I_s^*+\gamma_2 e^{-\mu\tau_2}I_a^*}\left(5-\frac{1}{x_1}-\frac{x_1}{x_2}-\frac{x_3}{x_4}-\frac{x_4}{x_6}-\frac{x_6}{x_3}x_2\right)\\
&+\frac{\beta(1-\rho)(1-\phi)\gamma_1 e^{-(\mu+d_1)\tau_2}I_s^*Q^*S_L^*}{\gamma_1 e^{-(\mu+d_1)\tau_2}I_s^*+\gamma_2 e^{-\mu\tau_2}I_a^*}\left(5-\frac{1}{x_1}-\frac{x_1}{x_2}-\frac{x_3}{x_5}-\frac{x_5}{x_6}-\frac{x_6}{x_3}x_2\right),
\end{aligned}
\tag{2.22}
$$

where $x_1=\frac{S_H}{S_H^*}$, $x_2=\frac{S_L}{S_L^*}$, $x_3=\frac{E}{E^*}$, $x_4=\frac{I_s}{I_s^*}$, $x_5=\frac{I_a}{I_a^*}$, and $x_6=\frac{Q}{Q^*}$. It follows that if $x_i=1$, (for $i=1,2,3,4,5$), that is., $S_H=S_H^*$, $S_L=S_L^*$, $E=E^*$, $I_s=I_s^*$, $I_a=I_a^*$ and $Q=Q^*$ we have $W_1'(t)=0$. Furthermore, since the arithmetic mean is greater or equal to the geometric mean, that is; $x_1+\frac{1}{x_1}\geq 2\sqrt{x_1\cdot\frac{1}{x_1}}$, it implies $W_1'(t)\leq 0$. Using the LaSalle's invariance principle [29], we conclude that the endemic equilibrium point $\mathcal{E}^*$ of system (2.1)-(2.8) is globally asymptotically stable if $\mathcal{R}_0>1$. This completes the proof. □

2.4 Model Parameterization

To numerically simulate system (2.1)-(2.8) we will calibrate the model using parameter values in literature (see Table 1) and validate it with observed COVID-19 cases for Wuhan, China presented in [30]. On fitting the model with data, we made use of the least squares curve fit routine (lsqcurvefit) in MATLAB with optimization to estimate our unknown parameters. We let the cumulative new infections predicted by our model, $C(t)$ to be solutions (2.24) of the equation:

$$
C'(t)=\gamma_1 e^{-(\mu+d_1)\tau_2}I_s(t-\tau_2)+\gamma_2 e^{-\mu\tau_2}I_a(t-\tau_2). \tag{2.23}
$$

IJMSO

International Journal of Mathematical Sciences and Optimization: Theory and Applications
11(3), 2025, Pages 88 - 107
https://doi.org/10.5281/zenodo.17604615

Thus, the estimation of confirmed cumulative cases for COVID-19 over a defined time frame $t_{k-1} \leq t \leq t_k$ (where t_{k-1} and t_k represents the beginning and end of the time interval, respectively) from the model output requires to compute:

$$\int_{t_{k-1}}^{t_k} C(t)dt. \tag{2.24}$$

During the fitting process we set initial population levels to: $S_H(0) = 4000$, $S_L(0) = 0$, $E(0) = 20$, $I_s(0) = 20$, $I_a(0) = 10$, $Q(0) = 6$, $R(0) = 0$. Simulation results of the model fitting are depicted in Fig. 2. Results show that the model predictions are close to the observed values, particularly during the first 36 days and on the last 4 days, the model slightly underestimated the observed cases.

Table 1: Parameters and values

Symbol	Description	Value	Units	Source
Λ	Per capita human recruitment rate	Day $^{-1}$	20	[32]
d_1, d_2	Disease induced deaths rate	Day $^{-1}$	0.005	[33]
μ	Natural deaths rate	Day $^{-1}$	5×10^{-6}	[33]
β	Disease transmission rate	Day $^{-1}$	5.4×10^{-6}	Fitting
α^{-1}	Incubation period	Day	$2(2-14)$	[32]
ϕ	Vaccine efficacy	Dimensionless	0.5 (0-1)	[32]
σ	Rate of vaccination	Day $^{-1}$	0.03	[32]
p	Proportion of exposed individuals who develop clinical signs of the disease	Dimensionless	0.75	[31]
γ_1	Rate of hospitalization of clinical patients	Day^{-1}	0.94	1001[32]
γ_2	Rate of hospitalization of asymptomatic patients	Day^{-1}	0.94	1001[32]
r_1	Recover rate of symptomatic infectious individuals	Day^{-1}	0.015	1001[32]
r_2	Recover rate of asymptomatic infectious individuals	Day^{-1}	0.004	1001[32]
δ	Recover rate of hospitalized humans	Day^{-1}	0.5	1001[32]
ψ	Reduction of infectivity asymptomatic individuals	Dimensionless	$0.6[0,1)$	Fitting
ρ	Reduction of infectivity hospitalized patients	Dimensionless	$0.9[0,1)$	Fitting
τ_1	Time taken by susceptible individuals to take a vaccine	Days	$30[0,300)$	Fitting
τ_2	Time taken to detected and hospitalize an infectious individual	Days	$5[0,10)$	Fitting

2.5 Sensitivity analysis of the reproduction number

The reproduction number is a crucial threshold quantity in modelling infectious diseases. It illustrates the strength of the disease to persist or die out. Therefore, it is essential to investigate the relationship between the reproduction number and model parameters that define it. Various approaches can be utilized; however, the partial rank correlation coefficient (PRCC) is one of the techniques that has been widely used by several researchers. Comprehensive information on PRCC can be found in [34]. In a nutshell, a PRCC allows one to investigate the correlation between the reproduction number and the model parameters while all parameters are varied simultaneously across their defined range of possible values. The PRCC output for $\mathcal{R}_0$ of system (2.1)-(2.8) is depicted in Fig. 3. From the PRCC output (Fig. 3) one can observe that $\mathcal{R}_0$ is strongly sensitive to vaccine efficacy (ϕ), disease transmission rate (β) and recruitment rate (Λ). Thus, use of vaccines with high efficacy significantly reduces disease transmission potential. In addition, we can observe that an increase in disease transmission rate will significantly increase $\mathcal{R}_0$. Thus, other disease control measures such as social distancing and use of face masks that have proved to be capable of reducing transmission could be essential to mitigate the spread of the disease.

IJMSO
International Journal of Mathematical Sciences and Optimization: Theory and Applications
11(3), 2025, Pages 88 - 107
https://doi.org/10.5281/zenodo.17604615

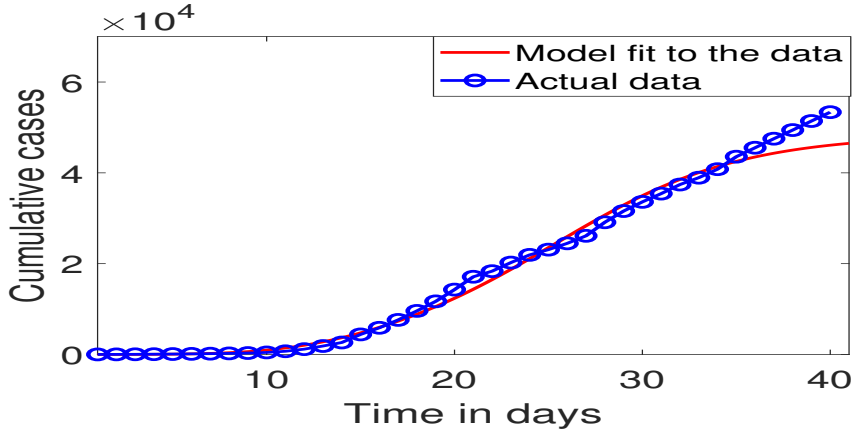

Figure 2: Simulation results showing the model estimates versus the observed cases.

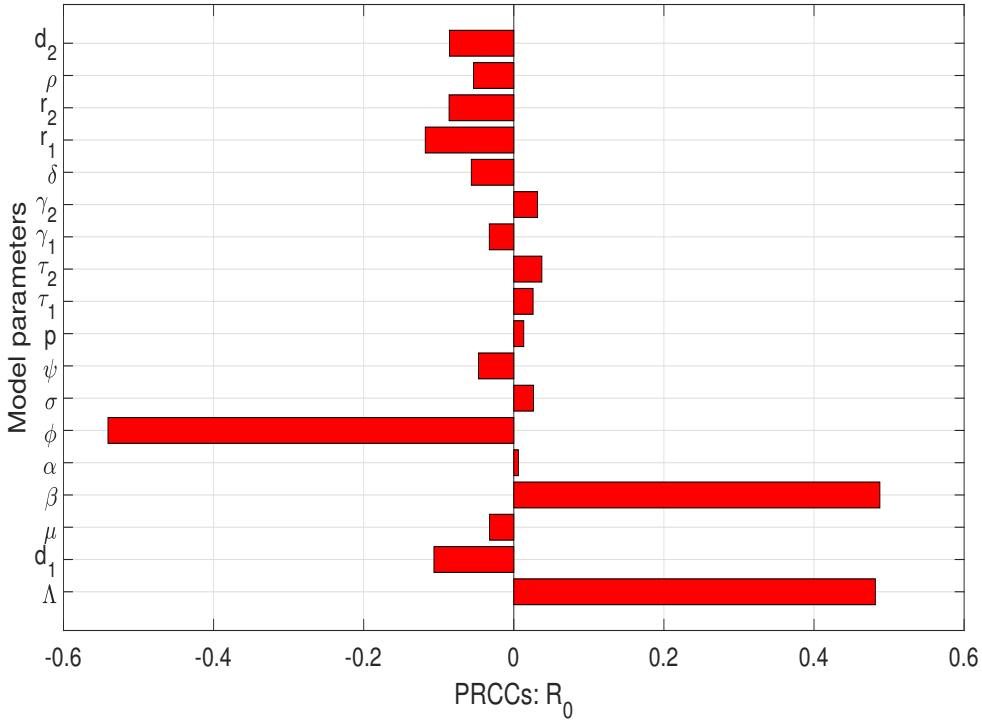

Figure 3: Sensitivity analysis of $\mathcal{R}_0$ with respect to model parameters

2.6 Dynamical behavior of model solutions over time

In this section, we numerically investigated the stability of system (2.1)-(2.8). We simulated system (2.1)-(2.8) for $\mathcal{R}_0 < 1$ and $\mathcal{R}_0 > 1$, and the results are illustrated in Fig. 4, 5 and 6, respectively. Simulation results in Fig. 4 show that whenever $\mathcal{R}_0 < 1$, model solutions converge to the origin. This implies that whenever $\mathcal{R}_0 < 1$ the disease dies out. These results concur with analytical results summarized by Theorem 2.2. However, in Fig. 5 and 6 one can observe that when $\mathcal{R}_0 > 1$, model solutions commence with periodic oscillation which will eventually die out with time leading convergence of solutions to a unique endemic equilibrium point. Since all the model solutions for

IJMSO
International Journal of Mathematical Sciences and Optimization: Theory and Applications
11(3), 2025, Pages 88 - 107
https://doi.org/10.5281/zenodo.17604615

the infected compartments stabilize above the origin it implies that whenever $\mathcal{R}_0 > 1$, the disease persists. This outcome agrees with findings summarized by Theorem 2.3.

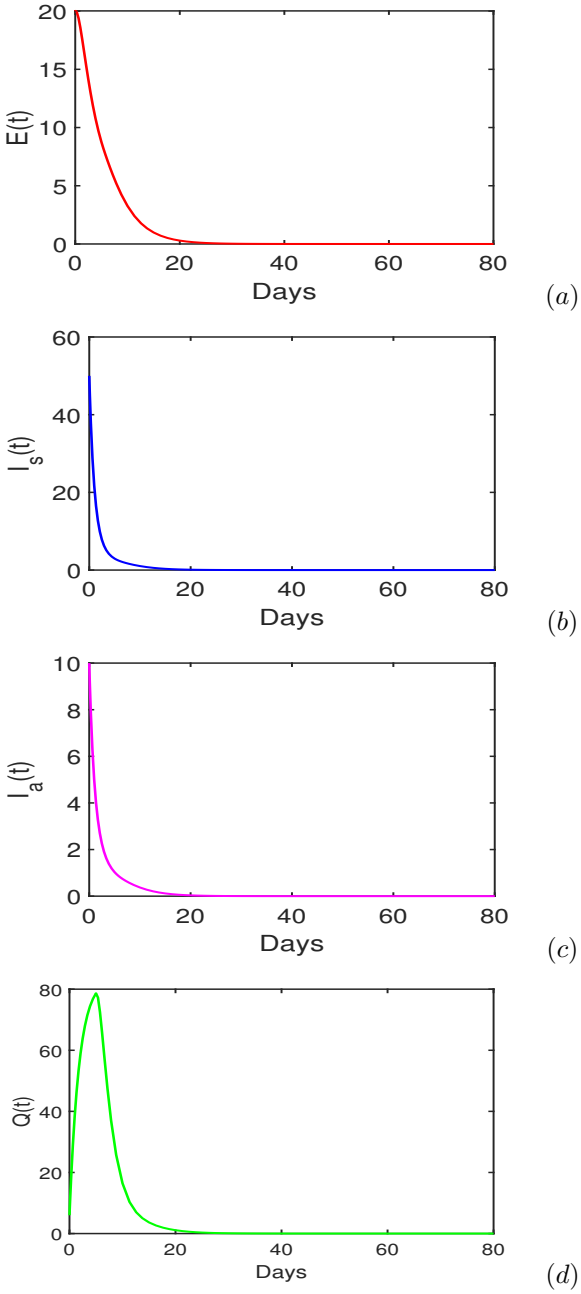

Figure 4: Solutions of (2.1)-(2.8) for infected compartments with $\mathcal{R}_0 < 1$. We set $\tau_1 = 10$ days and $\tau_2 = 5$ days.

2.7 Effects of vaccine hesitancy on disease dynamics

To quantitatively and qualitatively examine the influence of vaccine hesitancy on the evolution of the disease, we fixed τ_2 simulated system (2.1)-(2.8) with different values of τ_1. The output is shown in Fig. 7 and 8). Simulation results in both scenarios (Fig. 7 and 8) show that vaccine hesitancy

IJMSO
International Journal of Mathematical Sciences and Optimization: Theory and Applications
11(3), 2025, Pages 88 - 107
https://doi.org/10.5281/zenodo.17604615

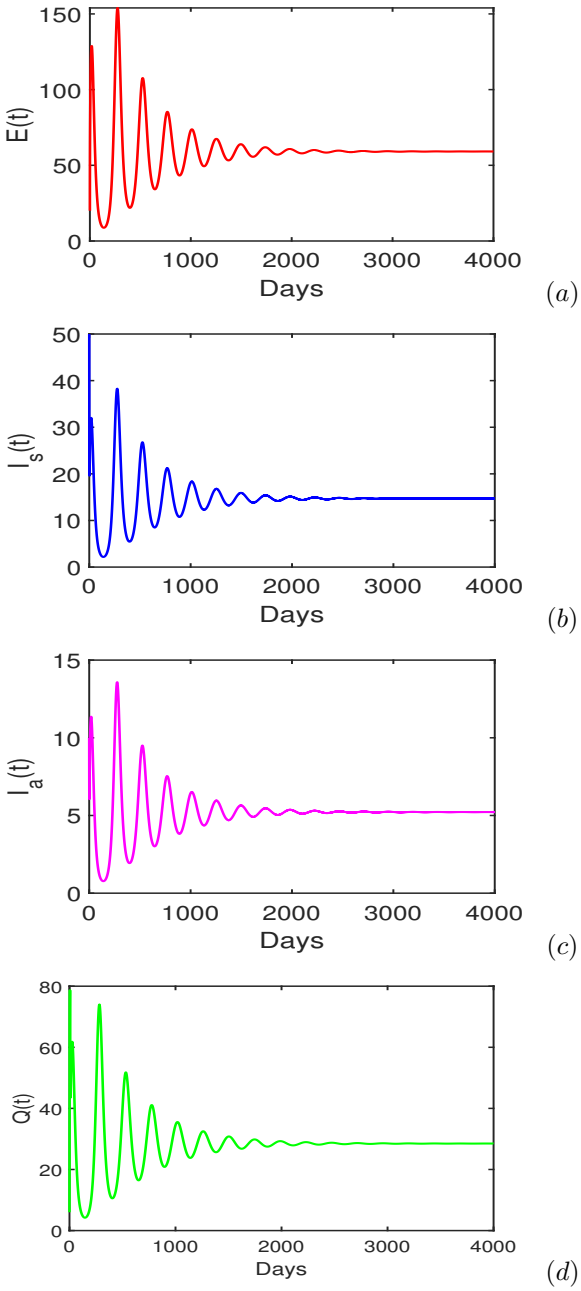

Figure 5: Solutions of (2.1)-(2.8) for infected compartments with $\mathcal{R}_0 > 1$. We set $\tau_1 = 10$ days and $\tau_2 = 5$ days.

influences the evolution of the disease. We can observe that vaccine hesitancy leads to oscillating model solutions. The oscillations represent disease waves. The oscillations are more pronounced for $0 \leq t \leq 1000$, thereafter they fade away, leading the solutions to converge at the unique endemic equilibrium point. We can also observe that as τ_1 increases, the time required for the infections to reach the peak increases.

IJMSO
International Journal of Mathematical Sciences and Optimization: Theory and Applications
11(3), 2025, Pages 88 - 107
https://doi.org/10.5281/zenodo.17604615

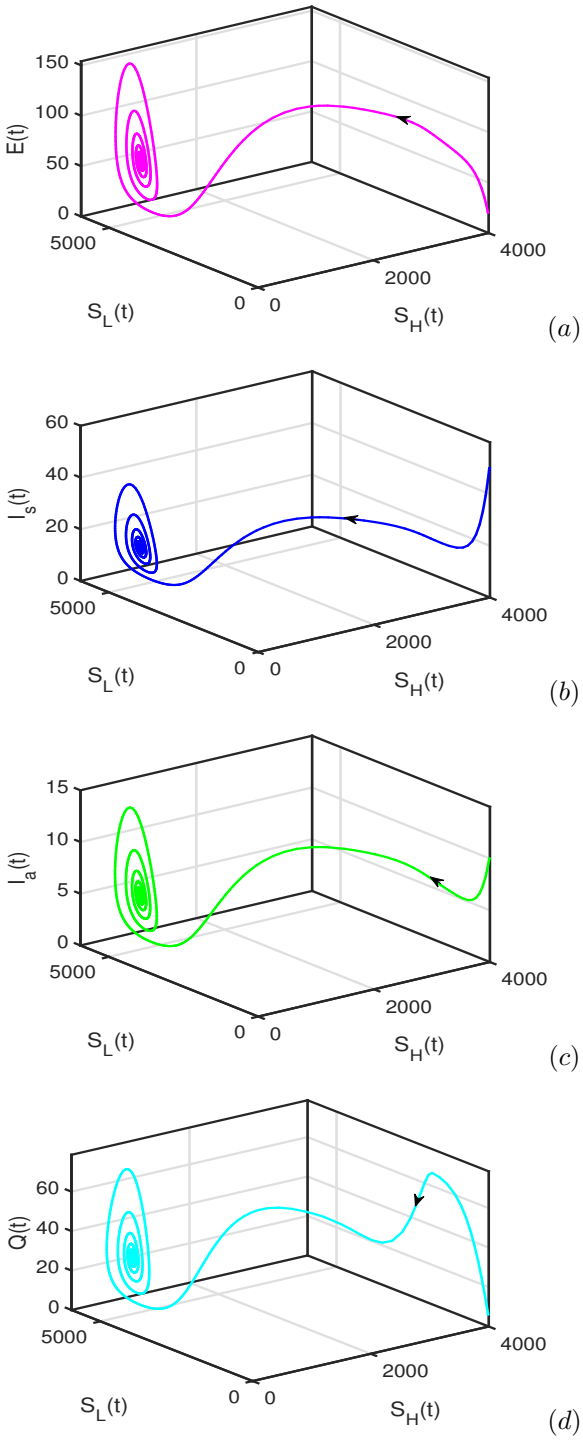

Figure 6: Solutions of (2.1)-(2.8) for infected compartments with $\mathcal{R}_0 > 1$. We set $\tau_1 = 10$ days and $\tau_2 = 5$ days.

IJMSO
International Journal of Mathematical Sciences and Optimization: Theory and Applications
11(3), 2025, Pages 88 - 107
https://doi.org/10.5281/zenodo.17604615

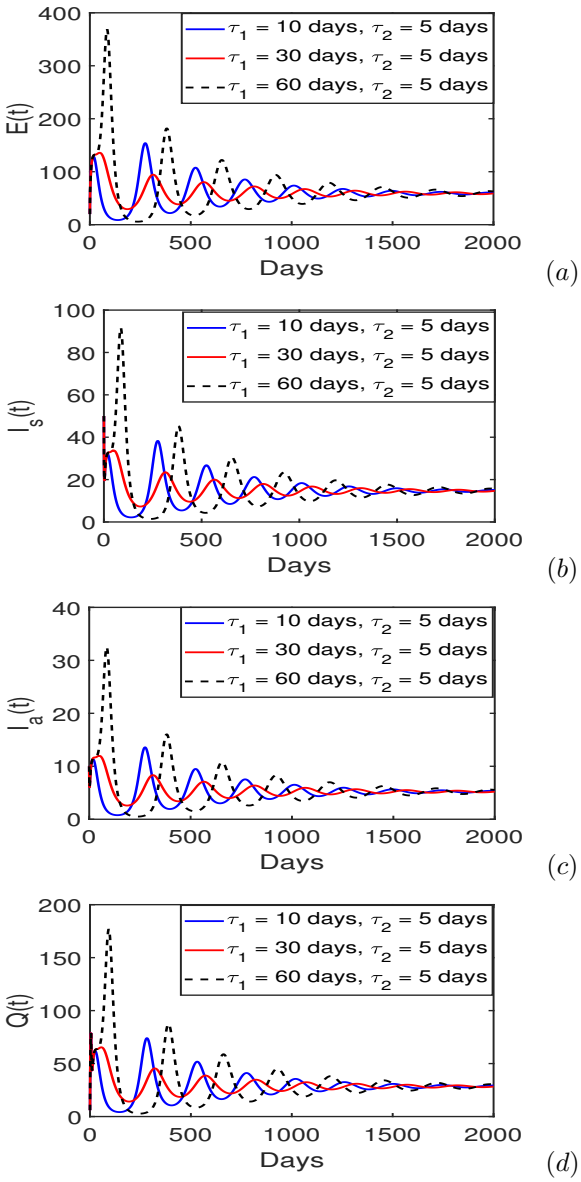

Figure 7: Effects of varying vaccine hesitancy on disease dynamics.

2.8 Public health implications of delays in screening of infectious individuals

We numerically characterized the effects of delaying screening of clinically infected individuals by simulating system (2.1)-(2.8) at different values of τ_2 while τ_1 is fixed (see Fig. 9). Simulation results suggest that delays in screening clinical patient results in periodic oscillations as observed with vaccine hesitancy. However, oscillations associated with τ_2 do not have a large amplitude compared to those associated with τ_1. Furthermore, increasing τ_2 does not remarkably increase the time taken by the disease to reach its peak as compared to when τ_1 is increased. Based on these outcomes, we propose that vaccine hesitancy has a stronger public health impact compared to the screening of clinically infected individuals.

IJMSO
International Journal of Mathematical Sciences and Optimization: Theory and Applications
11(3), 2025, Pages 88 - 107
https://doi.org/10.5281/zenodo.17604615

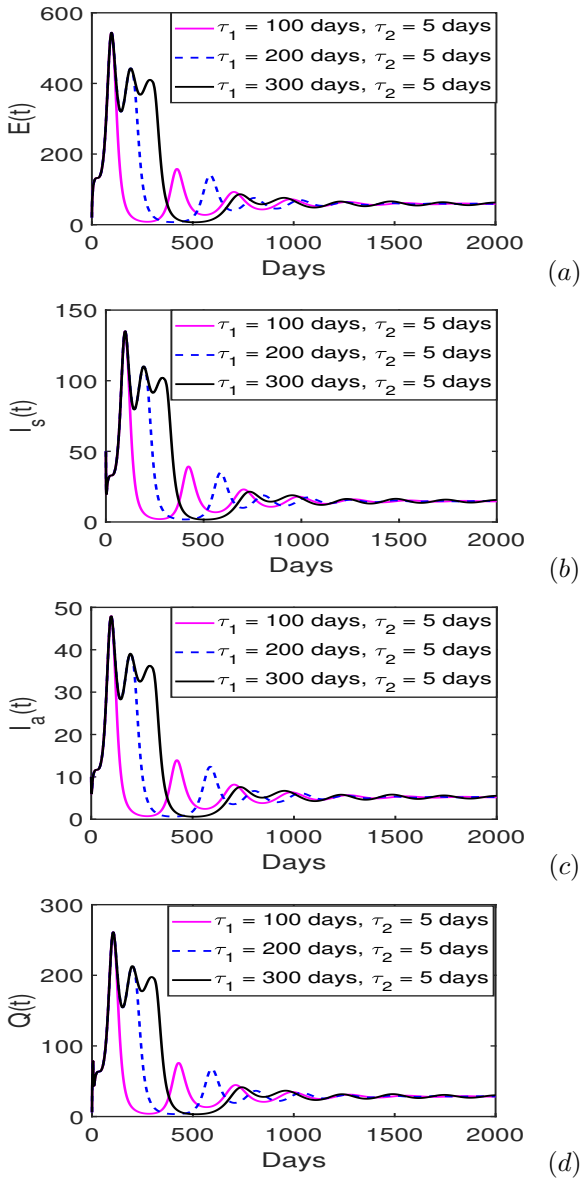

Figure 8: Effects of varying vaccine hesitancy on disease dynamics.

2.9 Implications of vaccine hesitancy and delays in screening clinically infected individuals

We investigated the influence of both vaccine hesitancy and delays in screening clinically infected individuals through simulating (2.1)-(2.8) at different values of τ_1 and τ_2. The output is in Fig. 10. As one can observe, the results concur with earlier findings that delays in accepting vaccination and screening of clinically infected individuals lead to periodic oscillations, which will eventually fade over time. This shows that vaccine hesitancy and screening of clinically infected individuals have a strong influence on the evolution of the disease and have the potential to result in outbreaks.

IJMSO
International Journal of Mathematical Sciences and Optimization: Theory and Applications
11(3), 2025, Pages 88 - 107
https://doi.org/10.5281/zenodo.17604615

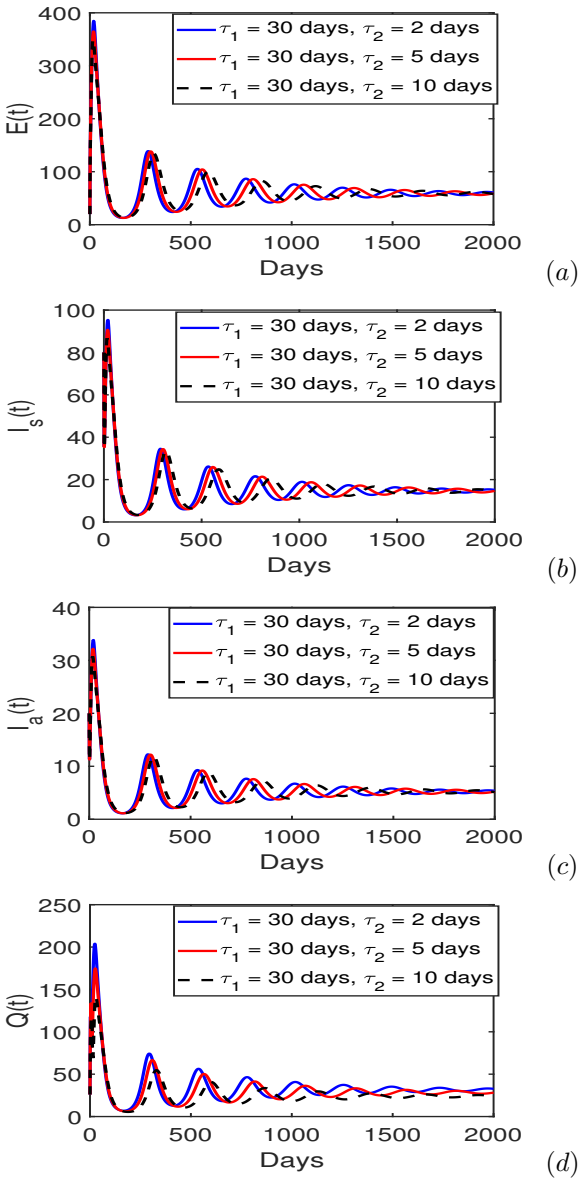

Figure 9: Effects of delayed screening of infectious individuals on disease dynamics.

3 Conclusion and Recommendations

In this paper, we have developed a mathematical model of COVID-19 that integrates critical factors such as vaccine hesitancy and delays in screening infectious individuals. Our analysis revealed two steady states: a disease-free equilibrium and an endemic equilibrium, both of which exhibit global stability depending on the reproductive number. Through extensive numerical experiments, we established that vaccine hesitancy leads to periodic oscillations in disease dynamics, with a notable increase in the time to peak infection as vaccine acceptance delays extend. Conversely, while delays in screening also affect the disease trajectory, they do not significantly alter the timing of peak infection. A key insight from our findings is the pronounced impact of vaccine hesitancy on public health compared to delays in screening. The amplitude of oscillations associated with vaccine hesitancy suggests that addressing this issue could be more critical in managing the spread

IJMSO
International Journal of Mathematical Sciences and Optimization: Theory and Applications
11(3), 2025, Pages 88 - 107
https://doi.org/10.5281/zenodo.17604615

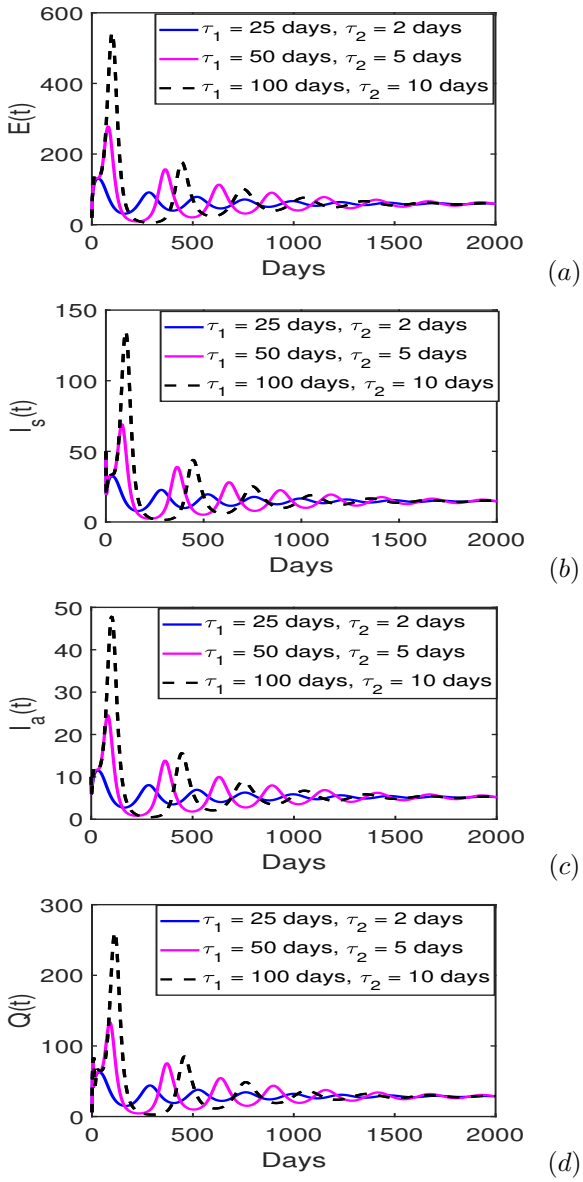

Figure 10: Combined effects of vaccine hesitancy and delayed screening of infectious individuals on disease dynamics.

of infectious diseases. This highlights the need for targeted interventions that focus on improving vaccine acceptance, as it may play a more pivotal role in controlling outbreaks than previously recognized.

To address these challenges, we recommend several strategic actions. First, enhancing public awareness campaigns is essential. Developing and implementing robust public health initiatives aimed at reducing vaccine hesitancy will be vital. These campaigns should leverage social media, community outreach, and trusted local figures to convey accurate information about vaccine safety and efficacy. Furthermore, it is crucial to monitor and address miscommunication effectively. Establishing monitoring systems to identify and counter misinformation related to vaccines, especially during health crises, can mitigate the impact of false narratives. Collaborating with media outlets to promote factual reporting will be instrumental in this effort. In addition, while our findings

suggest that screening delays may not significantly affect peak infection timing, it remains essential to integrate screening protocols. Timely identification and isolation of infectious individuals are crucial. Health authorities should ensure that screening processes are efficient and accessible to minimize transmission risks. Looking forward, further research should investigate additional socio-economic and psychological factors influencing vaccine hesitancy. Understanding the role of media narratives and community trust can inform more effective strategies for public health interventions, enhancing our ability to combat misinformation and improve vaccine uptake. Lastly, policy implications should be prioritized. Policymakers must allocate funding for initiatives that increase vaccine uptake and improve screening processes. By adopting this dual approach, we can enhance overall public health outcomes during infectious disease outbreaks and foster more resilient communities.

References

[1] Muhajarine, N., Adeyinka, D. A., McCutcheon, J., Green, K. L., Fahlman, M., & Kallio, N. (2021). COVID-19 vaccine hesitancy and refusal and associated factors in an adult population in Saskatchewan, Canada: Evidence from predictive modelling. PLoS ONE, 16(11), e0259513. DOI: 10.1371/ journal.pone.0259513

[2] Suneja, M., Beekmann, S.E., Dhaliwal, G., Miller, A. C., & Polgreen, P. M. (2022). Diagnostic delays in infectious diseases. Diagnosis (Berl), 9(3), 332-339. DOI: 10.1515/dx-2021-0092

[3] Aw, J., Seng, J.J.B., Seah, S.S.Y., & Low, L.L. (2021). COVID-19 Vaccine HesitancyA Scoping Review of Literature in High-Income Countries. Vaccines, 9(8), 900. DOI: 10.3390/vaccines9080900

[4] Dhama, K., Sharun, K., Tiwari, R., Dhawan, M., Emran, T. B., Rabaan, A. A., & Alhumaid, S. (2021). COVID-19 vaccine hesitancy-reasons and solutions to achieve a successful global vaccination campaign to tackle the ongoing pandemic. Human Vaccines & Immunotherapeutics, 17(10), 3495-3499. DOI: 10.1080/21645515.2021.1926183

[5] Pourrazavi, S., Fathifar, Z., Sharma, M., & Allahverdipour, H. (2023). COVID-19 vaccine hesitancy: A Systematic review of cognitive determinants. Health Promotion Perspectives, 13(1), 21-35. DOI: 10.34172/hpp.2023.03

[6] Yörük, S., & Güler, D. (2021). Factors associated with pediatric vaccine hesitancy of parents: A cross-sectional study in Turkey. Human Vaccines & Immunotherapeutics, 17(11), 4505-4511. DOI: 10.1080/21645515.2021.1953348

[7] Romer, D., Jamieson, K. H., & Kligler-Vilenchik, L. (2022). Misinformation about vaccine safety and uptake of COVID-19 vaccines among adults and 5-11-year-olds in the United States. Vaccine, 40(45), 6463-6470. DOI: 10.1016/j.vaccine.2022.09.046

[8] Kelemu, B., Tariku, A., Diriba, G., & Gelibo, T. (2024). Global COVID-19 Vaccine acceptance level and its determinants: An umbrella review. BMC Public Health, 24(1), 5. DOI: 10.1186/s12889-023-17497-4

[9] Elharakeh, A., Thakur, N., Quader, S., Hashmi, F. K., Saleem, A., Zeeshan, M., & Riaz, M. (2021). COVID-19 Vaccine Hesitancy Worldwide: A Concise Systematic Review of Vaccine Acceptance Rates. Vaccines, 9(2), 160. DOI: 10.3390/vaccines.902016

[10] Sauro, K., Vatanpour S., Thomas, A., et al. (2024). Consequences of delaying non-urgent surgeries during COVID-19: A population-based retrospective cohort study in Alberta, Canada. BMJ Open 2024 (14), e085247. DOI: 10.1136/bmjopen-2024-085247

[11] Olanipekun, T. (2021). The impact of COVID-19 testing on length of hospital stay and patient flow in hospitals. Journal of Community Hospital Internal Medicine Perspectives, 11(2), 180-183. DOI: 10.1080/20009666.2020.1866249

[12] Motta, M., Callaghan, T., Padmanabhan, M. (2025). Quantifying the prevalence and determinants of respiratory syncytial virus (RSV) vaccine hesitancy in US adults aged 60 or older. Public Health, 238(40), 3-6. DOI: 10.1016/j.puhe.2024.08.004

[13] Carethers, J. M., Sengupta, R., Blakey, R., Ribas, A., & D'Souza, G. (2020). Disparities in Cancer Prevention in the COVID-19 Era. Cancer Prev Res (Phila), 13(11), 893-896. DOI: 10.1158/1940-6207.CAPR-20-0447

[14] Blumenthal, S. J., Goldenson, J., Gonzalez, A., Landefeld, C. S., & Krieger, N. (2021). Racial and ethnic inequities in the early distribution of U.S. COVID-19 testing sites and mortality. European Journal of Clinical Investigation, 51(11), e13669. DOI: 10.1111/eci.13669,

[15] Gashirai, T. B., Musekwa-Hove, S. D., Lolika, P. O., & Mushayabasa, S. (2020). Global stability and optimal control analysis of a foot-and-mouth disease model with vaccine failure and environmental transmission. Chaos Solitons and Fractals 132(2020), 109568. DOI: 10.1016/j.chaos.2019.109568.

[16] Faniran , T. S., & Ayoola , E. O. (2019). Mathematical Analysis of Basic Reproduction Number for the Spread and Control of Malaria Model with Non-Drug Compliant Humans. International Journal of Mathematical Sciences and Optimization: Theory and Applications, 2019(2), 558 - 570. https://ijmso.unilag.edu.ng/article/view/489

[17] Troiano, G., & Nardi, A. (2021). Vaccine hesitancy in the era of COVID-19, Public health, 194 (2021), 245-251. DOI: 10.1016/j.puhe.2021.02.025

[18] Müller, J., & Koopmann, B. (2016). The effect of delay on contact tracing, Math. Biosci. 282 (2016), 204-214. DOI: 10.1016/j.mbs.2016.10.010

[19] Lu, H., Ding, Y., Gong, S., & Wang, S. (2021). Mathematical modeling and dynamic analysis of SIQR model with delay for pandemic COVID-19. Math. Biosci. Eng., 18(4), 3197-3214. DOI: 10.3934/mbe.2021159

[20] Albani, V. V., Loria, J., Massad, E., & Zubelli, J. P. (2021). The impact of COVID-19 vaccination delay: A data-driven modeling analysis for Chicago and New York City. Vaccine 39(41), 6088-6094. DOI: 10.1016/j.vaccine.2021.08.098

[21] Yang, W. (2021). Modeling COVID-19 pandemic with hierarchical quarantine and time delay, Dyn. Games Appl., 11(4), 892-914. DOI: 10.1007/s13235-021-00382-3

[22] Frnak, B., Ethin-Osa (2021). A Laplace Decomposition Analysis of Corona Virus Disease 2019 (Covid 19) Pandemic Model. Interenational Journal of Mathematical Sciences and Optimization: Theory and Applications, 6(2), 847-861. DOI: 10.6084/m9.figshare.13643414

[23] Al-Tuwairqi, S. M., & Al-Harbi, S. K. (2022). A time-delayed model for the spresd of COVID-19 with vaccination. Scientific Reports, (2022) 12, 19435. DOI: 10.1038/s41598-022-23822-5

[24] Chen, T., Wu, D., Chen, H., Yan, W., Yang, D., Chen, G., Ma, K., Xu, D., Yu, H., & Wang, H. (2020). Clinical Characteristics of 113 deceaseed Pattients with coronavirus disease 2019: Retrospective study. BMJ (2020),368, m1091. DOI: 10.1136/bmj.m1091

[25] Wang, C., Horby, P. W., Hayden, F. G., & Gao, G. F. (2020). A novel coronavirus outbreak of global health concern. The Lancet, 395(10223), 470-473. DOI: 10.1016/S0140-6736(20)30185-9

[26] Rui Xu. Global stability of a delayed epidemic model with latent period and vaccination strategy. (2012). Applied Mathematical Modelling 36 (2012) 52935300. DOI: 10.1016/j.apm.2011.12.037

[27] Hale, J. K., & Verduyn Lunel, S. (1993). Introduction to Functional Differential Equations. Springer-Verlag, New York. DOI: 10.1007/978-1-4612-4342-7

[28] Van den, D.P., & Watmough, J. (2002). Reproduction numbers and sub-threshold endemic equilibria for compartmental models of disease transmission. Math. Biosci. 180 (2002), 29-48. DOI: 10.1016/s0025-5564(02)00108-6

[29] LaSalle, J. (1960). Some extensions of Liapunovâs second method, IRE Trans. Circuit Theory, 7(4), 520-527. DOI: 10.1109/tct.1960.1086720

[30] Faïçal, N., Iván, A., Juan, J. N., & Delfim, F. M. (2020). Mathematical modeling of COVID-19 transmission dynamics with a case study of Wuhan, Chaos Solit. Fractals 135 (2020) 109846. DOI: 10.1016/j.chaos.2020.109846

[31] Mushayabasa, S., Ngarakana-Gwasira, E. T., & Mushanyu, J. (2020). On the role of governmental action and individual reaction on COVID-19 dynamics in South Africa: A mathematical modelling study. Inform. Med. Unlocked 20 (2020) 100387. DOI: 10.1016/j.imu.2020.100387.

[32] Aatif, A., Saif, U., & Khan, M. A.(2022). The impact of vaccination on the modeling of COVID-19 dynamics: A fractional order model. Nonlinear Dyn., 110 (2022), 3921-3940. DOI: 10.1007/s11071-022-07798-5

[33] Abdul-Rahman, J. M., & Alfred, K. H. (2020). Mathematical modelling on COVID-19 transmission impacts with preventive measures: a case study of Tanzania, J. Biol. Dyn. 14 (2020), 748-766. DOI: 10.1080/17513758.2020.1823494.

[34] Marino, S., Hogue, I. B., Ray, C. J. R., & Kirschner, D. E. (2008). A methodology for performing global uncertainty and sensitivity analysis in systems biology, J. Theor. Biol. 254(1), 178-96. DOI: 10.1016/j.jtbi.2008.04.011